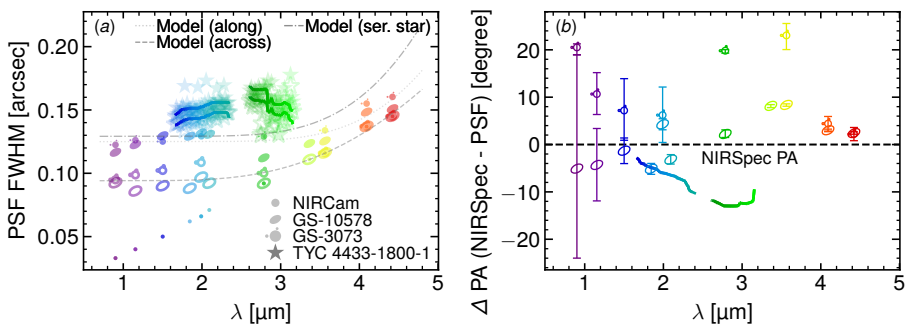




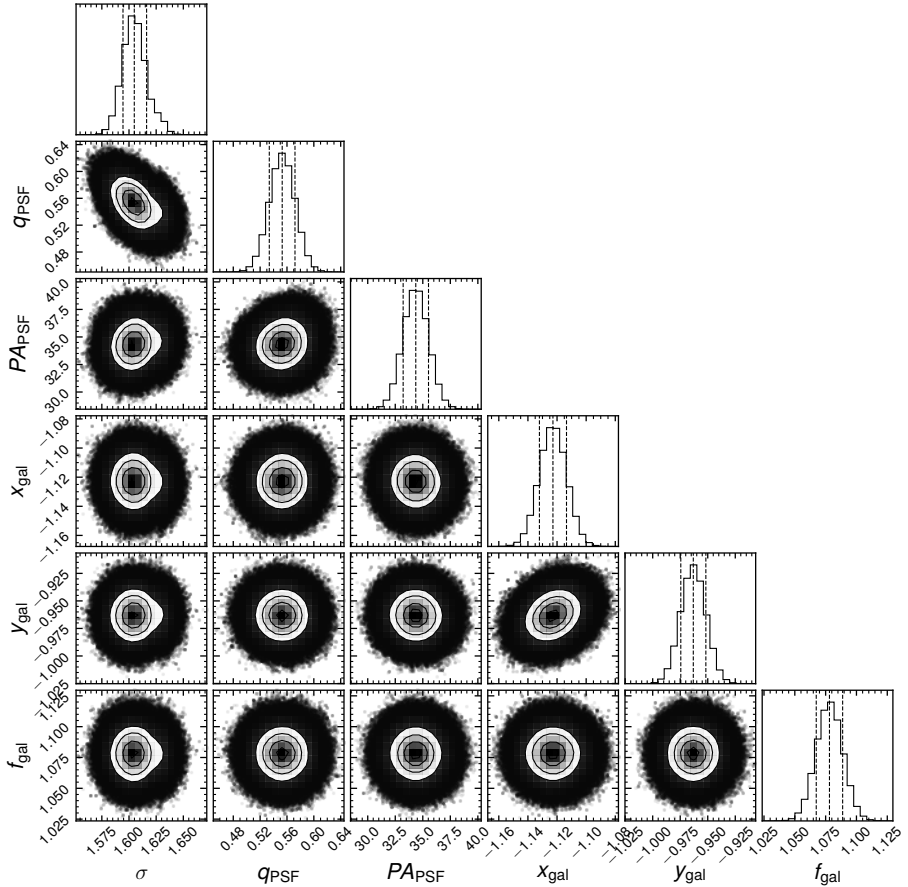
A fast-rotator post-starburst galaxy quenched by supermassive black-hole feedback at $z = 3$

In the format provided by the
authors and unedited

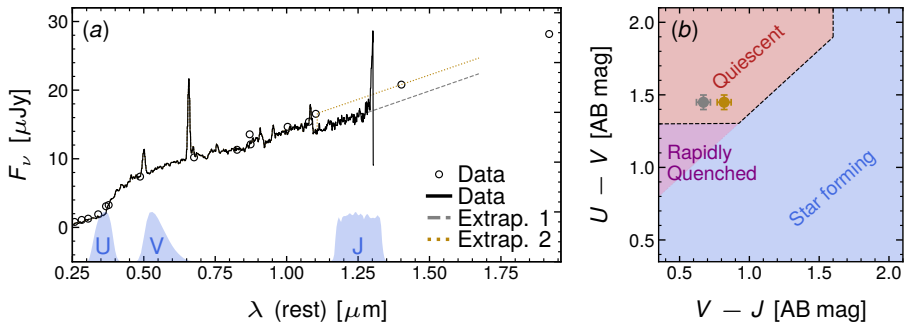
Supplementary Figures



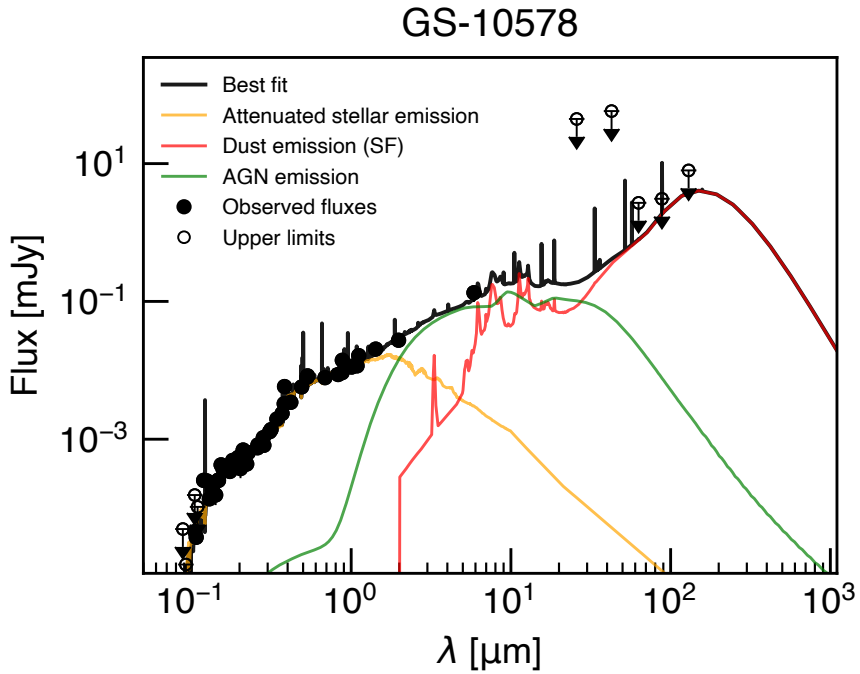
Supplementary Figure 1: Summary of the PSF determination from the reconstructed datacube. **Panel a.** PSF FWHM as a function of wavelength, using three methods. Method I (stars and solid lines) uses the calibration star TYC 4433-1800-1. Method II (dot-dashed line) uses the serendipitous star inside the NIRSpec/IFS field of view for the observations of GS-10578 (Eq. 1 in the main text). Method III uses NIRCcam wide- and medium-band imaging to model the PSF with a 2-d Gaussian with orthogonal axes, with one axis closer to the slice direction (filled symbols) and one closer to across slices (empty symbols); the dotted and dashed grey lines are analytical models of Method III, along and across slices, respectively (Eqs. 2 and 3 in the main text). The small dots show the FWHM of the NIRCcam empirical PSF for comparison. **Panel b.** Position angle of the PSF major axis (points with error bars, representing the median and 16th-84th inter-percentile range of the marginalised posterior probability distribution) compared to the NIRSpec position angle (dashed horizontal line). The major axis of the PSF is closer to the direction of the slices.



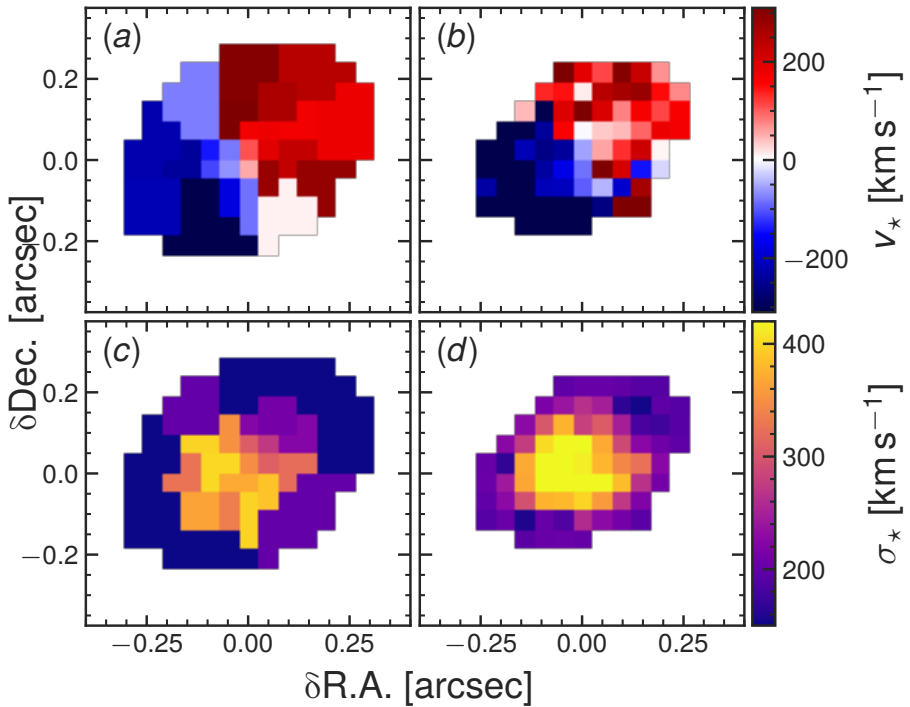
Supplementary Figure 2: Example posterior distribution for our PSF estimation based on matching NIRCcam imaging (method II). σ is the semi-major axis standard deviation of the Gaussian kernel we apply to the NIRCcam F182M imaging to best match NIRSpc. The kernel has axis ratio $q = 0.55$, but the NIRSpc/IFS PSF is the result of convolving this kernel with the NIRCcam PSF. The kernel position angle is 34° , meaning the NIRSpc/IFS PSF is elongated preferentially along the IFS slices.



Supplementary Figure 3: UVJ-diagnostic diagram of GS-10578. **Panel a.** NIRSpec prism spectrum (solid black) inside a 1.15-arcsec aperture, compared to *HST*, *JWST* and *Spitzer* photometry (circles). The dotted and dashed lines are different methods to extrapolate the NIRSpec data to extend to the *J*-band filter. **Panel b.** Position of GS-10578 in the UVJ diagram [1, highlighting two different measurements based on different extrapolations presented in panel a]. Regardless of the method used, our target falls in the quiescent region of the diagram (red), close to the demarcation of rapidly quenched galaxies (purple region). The 1- σ uncertainties are obtained by bootstrapping the data and repeating the measurement and extrapolation, with a systematic error floor of 0.05 mag.



Supplementary Figure 4: Spectral energy distribution fitting with CIGALE. The best-fit model (black) and the separate contributions of stars (yellow), host dust from the AGN (green) and star formation (red) are illustrated. The presence of a dust-obscured AGN is required by the MIR data from *Spitzer*/MIPS.



Supplementary Figure 5: Comparison of the stellar kinematics between two different methods. Results from the fiducial method (based on Voronoi bins, Method I) are in panels a and c. The alternative method (based on individual spaxel with constrained templates, Method II) is in panels b and d. The two measurements show good agreement, but the spaxel-by-spaxel fits tend to find higher σ_* in the centre, possibly due to lower S/N and smaller set of input templates for the fit.

References

- [1] Williams, R. J., Quadri, R. F., Franx, M., van Dokkum, P. & Labbé, I. Detection of Quiescent Galaxies in a Bicolor Sequence from $Z = 0-2$. *Astrophys. J.* **691** (2), 1879–1895 (2009). <https://doi.org/10.1088/0004-637X/691/2/1879>, <https://arxiv.org/abs/0806.0625> [astro-ph].